HHS Public Access

Author manuscript

Biochemistry. Author manuscript; available in PMC 2019 October 09.

Published in final edited form as:

Biochemistry. 2018 October 09; 57(40): 5910–5920. doi:10.1021/acs.biochem.8b00839.

Human eIF5 and eIF1A compete for binding to eIF5B

Kai Ying Lin[1], **Nabanita Nag**[1], **Tatyana V. Pestova**[2], and **Assen Marintchev**[*,1]

[1]Boston University School of Medicine, Dept. of Physiology & Biophysics, Boston, MA, 02118

[2]SUNY - Downstate Medical Center, Dept. of Cell Biology, Brooklyn, NY 11203

Abstract

Eukaryotic translation initiation is a multistep process requiring a number of eukaryotic translation initiation factors (eIFs). Two GTPases play key roles in the process. eIF2 brings the initiator Met-tRNA$_i$ to the pre-initiation complex (PIC). Upon start codon selection and GTP hydrolysis promoted by the GTPase-activating protein (GAP) eIF5, eIF2-GDP is displaced from Met-tRNA$_i$ by eIF5B-GTP and is released in complex with eIF5. eIF5B promotes ribosomal subunit joining, with the help of eIF1A. Upon subunit joining, eIF5B hydrolyzes GTP and is released together with eIF1A. We found that human eIF5 interacts with eIF5B and may help recruit eIF5B to the PIC. An eIF5B-binding motif was identified at the C-terminus of eIF5, similar to that found in eIF1A. Indeed, eIF5 competes with eIF1A for binding and has ~100-fold higher affinity for eIF5B. Since eIF5 is the GAP of eIF2, the newly discovered interaction offers a possible mechanism for coordination between the two steps in translation initiation controlled by GTPases: start codon selection and ribosomal subunit joining. Our results indicate that in human, eIF5B displacing eIF2 from Met-tRNA$_i$ upon subunit joining may be coupled to eIF1A displacing eIF5 from eIF5B, allowing the eIF5:eIF2-GDP complex to leave the ribosome.

Table of Contents

“Human eIF5 and eIF1A compete for binding to eIF5B”

Lin et al.

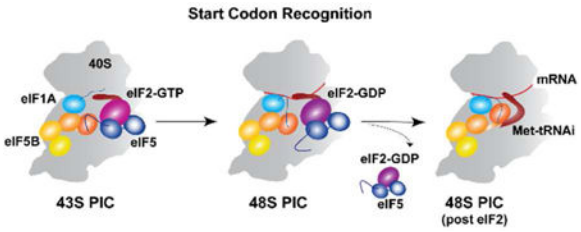

Keywords

translation initiation; eIF5B; eIF5; eIF1A; NMR

[*]Corresponding Author amarint@bu.edu., Phone: (617) 358-8486.

Supporting Information

Two Supplementary Figures and Supplementary References

Introduction

Translation initiation in eukaryotes consists of several steps: (i) 43S pre-initiation complex (PIC) assembly from the 40S ribosomal subunit and eukaryotic translation initiation factors (eIFs) 1, 1A, 2, 3, and 5, and the initiator Met-tRNA$_i$; (ii) recruitment of the 43S PIC to the 5'-end of mRNA by the cap-binding eIF4F complex; (iii) scanning along the mRNA; (iv) start codon selection; and (v) joining of the large ribosomal subunit. eIF2 is a GTPase that in its active, GTP-bound form, brings Met-tRNA$_i$ to the PIC. eIF5 is the GTPase-activating protein (GAP) of eIF2. eIFs 1,2, 3, and 5, as well as Met-tRNA$_i$, form a multifactor complex (MFC) off the ribosome and may bind to the PIC together, with the eIF5 C-terminal domain (eIF5-CTD) acting as the nucleating center for MFC assembly.[7] Basepairing between the anticodon of Met-tRNA$_i$ and the start codon induces major conformational changes in the PIC, from an open, scanning complex to a closed complex, locked at the start codon. The stringency of start codon selection is controlled by the interplay of several factors, including eIF1, which destabilizes PICs at non-AUG codons, AUG codons in suboptimal sequence context, or AUG codons too close to the 5'-end of mRNA (reviewed in references [8–13]).

The C-terminal tail (CTT) of eIF1A is located in the ribosomal P-site and counteracts the transition from open to closed complex. Start codon selection triggers the release of eIF1 from the PIC and "eviction" of eIF1A-CTT from the P-site.[1–3] eIF5 promotes GTP hydrolysis by eIF2, followed by phosphate release. eIF2-GDP has lower affinity for Met-tRNA$_i$ than eIF2-GTP, and is released together with its GAP, eIF5.[16–19] eIF2-GDP release is accelerated by a second GTPase, eIF5B,[20] which then itself binds to Met-tRNA$_i$. eIF5B-GTP, together with eIF1A, promotes ribosomal subunit joining, followed by GTP hydrolysis by eIF5B and release of eIF5B and eIF1A, leaving an 80S ribosome ready to start protein synthesis. An interaction between an eIF5B-binding motif, at the C-terminus of eIF1A, and domain 4 of eIF5B (eIF5B-D4) is important for both subunit joining and the coordinated release of eIF5B and eIF1A.[4, 21–23] This interaction is most likely established upon start codon selection, when eIF1A-CTT is displaced from the P-site and is thus able to contact eIF5B.

We recently reported that the binding affinity between eIF1A and eIF5B is regulated by a network of intramolecular interactions both within eIF1A and eIF5B. In particular, the intrinsically disordered eIF1A-CTT contacts dynamically the folded domain of eIF1A, which blocks the folded domain from interacting with domain 3 of eIF5B (eIF5B-D3) and weakens the binding of eIF1A-CTT to eIF5B-D4. eIF1A biding to the 40S ribosomal subunit disrupts the intramolecular interactions within eIF1A, increasing the affinity of eIF1A for eIF5B, when both proteins are bound to the ribosome.[6]

Here, we report that human eIF5, the GAP for eIF2, also binds to eIF5B, with affinity that is about two orders of magnitude higher than that of eIF1A. The interaction is mediated by an eIF5B-binding motif located at the C-terminus of eIF5, similar to that of eIF1A and the two proteins compete for binding to eIF5B. Since eIF5 is the GAP of eIF2, the newly discovered interaction links start codon selection and ribosomal subunit joining.

Materials and Methods

Protein expression and purification

The constructs used in this study are shown in Fig. 1. The proteins were cloned with an N-terminal GB1 tag, His_6-tag, and a TEV protease cleavage site (GH-tag). The expression and purification of human $eIF5B_{587–1220}$, (GH-ΔeIF5B); human $eIF5B_{951–1220}$, comprising domains 3 and 4 (GH-eIF5B-D34); and human $eIF5B_{1076–1220}$, comprising domain 4 (GH-eIF5B-D4) was as described previously.[6] Full-length human eIF5 (GH-eIF5) was expressed at 20 °C O/N and purified on a TALON Cell-Thru His-tag affinity column (Clontech) in buffer containing 20 mM Tris, pH 7.0, 300 mM KCl, 7 mM BME and 0.1 mM AEBSF. The GB1 tag was cleaved using TEV protease. Ion exchange chromatography on an Uno Q column was used to remove the GB1 tag as well as an abundant truncated fragment, corresponding to eIF5-NTD. $eIF5_{196–431}$ (GH-eIF5-CTD) was expressed and purified similarly to GH-eIF5. eIF5 fragments comprising the C-terminal 39 residues (GH-eIF5-CT39) and 9 residues (GH-eIF5-CT9) were expressed and purified similarly to GH-eIF5, but the expression was carried out at 37 °C for three hours. Fluorescein-labeled eIF1A-CT7 (Fl-eIF1A-CT7) and eIF5-CT7 (Fl-eIF5-CT7) were chemically synthesized. ^{15}N-, ^{13}C- and ^{2}H-labeling was achieved by growing bacteria on minimal medium supplemented with ^{15}N-NH_4Cl, ^{13}C-glucose, and ^{2}H-glucose + $^{2}H_2O$, respectively. Proteins were exchanged into Buffer A (20 mM Tris, pH 7.0, 150 mM KCl, 1 mM EDTA, 1 mM DTT and 0.1 mM AEBSF).

Fluorescence anisotropy

Fluorescence anisotropy (FA) measurements were done on a QuantaMaster QM4 fluorescent spectrometer (PTI), equipped with polarizers and dual monochromators. eIF5B-D4 and eIF5B-D34 were titrated into a synthetic fluorescein-labeled Fl-eIF1A-CT7 or Fl-eIF5-CT7 peptide, to determine their K_Ds for the peptide, by plotting FA as a function of protein concentration. The K_Ds of unlabeled eIF5 fragments for eIF5B-D4 and eIF5B-D34 were determined using a competition assay, where increasing concentrations of the unlabeled eIF5 fragment were titrated into a sample containing an eIF5B fragment and either Fl-eIF1A-CT7 or Fl-eIF5-CT7, plotting drop in FA as a function of unlabeled competitor concentration. The experiments were performed in a buffer containing 20 mM Tris–HCl, pH 7.0, 150 mM KCl, 1 mM EDTA, 1 mM DTT, 0.1 mM AEBSF, at 20 °C. Data analysis was done in SigmaPlot.

NMR

NMR experiments were performed in buffer A, containing 5% $^{2}H_2O$. NMR spectra were collected on a 500 MHz Bruker spectrometer with a cryoprobe (Boston University School of Medicine), except the Nuclear Overhauser Effect Spectroscopy (NOESY) spectra, which were collected on a 700 MHz Varian spectrometer (MIT), also with a cryoprobe. NMR resonance assignments for eIF5B-D4 were available.[4, 6] Resonance assignments for eIF5-CT39 and for the eIF5B-D4:eIF5-CT39 complex were obtained using standard triple-resonance experiments[24–27] on $^{15}N/^{13}C$-labeled samples. ^{15}N heteronuclear single-quantum coherence (HSQC) experiments on ^{15}N-labeled proteins were used for NMR binding analysis by Chemical Shift Perturbation (CSP) assay. For binding experiments, a ^{15}N-

labeled protein sample was titrated with increasing concentrations of unlabeled binding partner, until saturation (where no further chemical shift changes are observed), and affected residues were mapped on the surface of the protein. ^{15}N-edited NOESY-HSQC spectra were collected on eIF5B-D4:eIF5-CT39 complexes at 0.5 mM to 1 mM concentration. The proteins we mixed at 1.2 : 1 ratio of eIF5B-D4 to eIF5-CT39, at low protein concentration, followed by concentrating the samples in a 5K MW concentrator (Vivaspin). Excess free eIF5B-D4 (which has limited solubility) precipitated during concentration, yielding a stoichiometric ratio of eIF5B-D4 and eIF5-CT39, as confirmed by CSP analysis of the chemical shifts observed in an ^{15}N-HSQC spectrum. NOESY spectra were collected on three samples: ^{15}N-eIF5B-D4•^{15}N-eIF5-CT39, ^{15}N-eIF5B-D4•^{2}H/^{15}N-eIF5-CT39, and ^{2}H/^{15}N-eIF5B-D4•^{15}N-eIF5-CT39. In the first sample, the sidechains of both proteins are protonated and give rise to NOEs, both intra- and inter-molecular. In the second sample, only the sidechains in eIF5B-D4 are protonated and give rise to NOEs. Therefore, all sidechain NOEs to NHs in eIF5B-D4 are unambiguously **intra**-molecular (since they are to sidechains in the same protein) and all sidechain NOEs to NHs in eIF5-CT39 are unambiguously **inter**-molecular, since they are to sidechains in eIF5B-D4). This approach allows to readily and reliably identify **inter**-molecular NOEs. A model of the human eIF5B-D4:eIF5-CTT complex was generated based on the structure of the *S. cerevisiae* eIF5B:eIF1A-CTT complex.[5] All pairs of nuclei in eIF5B-D4 and eIF5-CT39, between which we had observed inter-molecular NOEs, were within less than seven Å of each other, even before optimizing sidechain orientations. Therefore, the structure of the human eIF5B-D4:eIF5-CTT complex is very similar to that of the *S. cerevisiae* eIF5B:eIF1A-CTT complex.[5]

Sequence analysis

Search for eIF5 and eIF1A sequences was done using PSI-BLAST[28] from NCBI (http://blast.ncbi.nlm.nih.gov/Blast.cgi). The results were then curated manually based on E-value and protein length, to eliminate incomplete sequences. The eIF5B-binding motif in eIF1A and eIF5 has limited information content; therefore, it was not possible to perform a reliable motif search. Instead, eIF1A and eIF5 sequences were inspected manually for the presence of the motif at their C-terminus. No obvious eIF5B-binding motifs were detected at the C-termini of proteins other than eIF1A and eIF5 (data not shown). Sequence alignment was done with ClustalW[29, 30] through the Max-Planck Institute for Developmental Biology Bioinformatics Toolkit (http://toolkit.tuebingen.mpg.de/).

Results

eIF5 binds to eIF5B and competes with eIF1A for binding

We have reported previously that eIF5B purified from mammalian cell lysates has weak eIF5-like activity *in vitro*[31] and noticed that endogenous eIF5B is contaminated with eIF5. Since this observation indicates that eIF5 and eIF5B likely bind directly to each other, we set out to map the interacting regions of the two proteins. Using His-tag affinity pull-down (data not shown), we found that eIF5 binds to recombinant eIF5B$_{\Delta 1–587}$ (corresponding to the entire archaeal aIF5B). We further mapped the interaction to the 39-residue eIF5 C-terminal tail (eIF5-CT39) and the eIF5B-D4 (the domain structure of the proteins and the constructs

used in this study are shown in Fig. 1). We used fluorescence anisotropy (FA) assay to determine the binding affinities of a set of eIF5 fragments for eIF5B and to further map the interacting regions (Fig. 2). The assay measures the displacement of a fluorescently labeled peptide from its binding site on a protein, by increasing concentrations of unlabeled peptides or proteins competing for the same binding site. We noticed that the C-terminus of human eIF5 resembles the C-terminus of eIF1A, which has been shown by us and others to bind to eIF5B-D4[4–6, 23] (see also Fig. 3, below). We found that eIF5-CTT does indeed compete with eIF1A-CTT for binding to eIF5B-D4 (data not shown), and the last seven residues of human eIF5 are sufficient for binding (Fig. 2 and Table 1), as in eIF1A.[6] The presence of eIF5B-D3 lowered the affinity of the interaction between eIF5B-D4 and eIF5 two-fold, also similar to eIF1A binding to eIF5B (Table 1).[6] Remarkably, eIF5-CT7 had ten-fold higher affinity for eIF5B than eIF1A-CT7. Furthermore, while the entire eIF1A-CTT has similar affinity to that of eIF1A-CT7 and full-length eIF1A has lower affinity due to competing intramolecular contacts, the complete eIF5-CTT has three-fold greater affinity than eIF5-CT7, and full-length eIF5 has the same or even slightly higher affinity. As a result, eIF5 has 100-fold greater affinity for eIF5B than eIF1A (Table 1).

Evolutionary conservation of the eIF5B-binding motif in eIF1A and eIF5

Analysis of the available eIF1A and eIF5 sequences shows that the eIF5B-binding site at the C-terminus of eIF1A is conserved in virtually all eIF1A homologs. The eIF5-CTT is conserved in *Metazoa*, but absent in eIF5 sequences from most fungi, including budding and fission yeast (a select set of eIF1A-CTT and eIF5-CTT sequences is shown in Fig. 3). A C-terminal tail with the eIF5B-binding signature is found in some fungal species from the subdivision *Ustilagomycotina*, including *Ustilago maydis*. The sequence of this motif is somewhat divergent from that of the typical motif found in most eIF1A and eIF5 sequences, in that it has leucines, instead of isoleucines. Interestingly, in these fungal species, the eIF1A C-terminus also has leucines, instead of isoleucines (Fig. 3). The functional significance of this difference is not clear, and we were unable to find obvious complementary changes in the eIF5B sequences from these organisms (data not shown). While no known plant eIF5 sequences have the eIF5B-binding motif, eIF5 sequences from species belonging to three other Kingdoms, *Alveolata*, *Excavata*, and *Protozoa*, have C-terminal tails with an eIF5B-binding motif. These motifs have similar consensus sequence to those of Metazoan eIF5 (Fig. 3). The eIF5B-binding motif is found in eIF5 sequences from individual branches of two phyla from Kingdom *Alveolata: Ciliophora (*Ciliates*)* and *Apicomplexa*. Among *Apicomplexa* members, all known *Plasmodium* and *Cryptosporidium* eIF5 sequences have the motif, whereas *Toxoplasma* species (which belong to the same order as *Cryptosporidium,* but a different family) do not. The situation is similar in Ciliates, where only part of the known eIF5 sequences have the eIF5B-binding motif. Only a limited number of protein sequences are available for the other Kingdoms. Three eIF5 sequences are available from species belonging to Class *Parabasalia*, Kingdom *Excavata*, all of which contain the eIF5B-binding motif, including *Trichomonas vaginalis* eIF5 (Fig. 3). Among *Protozoa* species, *Acanthamoeba castellanii,* from Class *Discosea,* Phylum *Amoebozoa*, has an eIF5B-bindig motif, whereas the other available eiF5 sequences (belonging to different classes of Phylum *Amoebozoa*) do not.

Mapping the eIF5-CTT•eIF5B-D4 interface by NMR

We mapped the binding interface between eIF5-CT39 and eIF5B-D4 using NMR chemical shift perturbation (CSP) assay (Fig. 4). In this experiment, the NMR spectrum of a protein labeled with an appropriate stable isotope (e.g. ^{15}N) is compared to the spectrum in the presence of an unlabeled (and thus "invisible") binding partner. The NMR chemical shifts are highly sensitive to the environment and, therefore, the peaks corresponding to residues affected by the interaction "move" upon binding. We used ^{1}H-^{15}N Heteronuclear Single-Quantum Coherence (HSQC) NMR spectra, which yield a peak for every NH group and thus serve as a "fingerprint" for a protein. To map the affected residues on the protein structures, we obtained the backbone NMR assignments for eIF5-CT39 using standard triple-resonance experiments.[24–27] The backbone assignments for eIF5B-D4 were already available from previous work.[4, 6] Our NMR experiments showed that eIF5-CT39 in the absence of interacting partner is unfolded, similar to eIF1A-CTT.[32] The NMR CSP assay identified the extreme C-terminus of eIF5-CTT as the primary binding site for eIF5B-CTD (Fig. 4A). Smaller effects were also observed in residues farther away from the C-terminus of eIF5, consistent with the FA results that eIF5-CT39 has slightly higher affinity for eIF5B-D4 than eIF5-CT7 (Table 1). However, only the residues near the C-terminus became folded upon binding to eIF5B, whereas the rest of eIF5-CT39 remained unstructured, indicating that this region of eIF5-CTT forms only weak, dynamic contacts with eIF5B-D4. Mapping the effects of eIF5-CT39 binding to ^{15}N-labeled eIF5B-D4 (Fig. 4B) indicated that the main eIF5-binding surface on eIF5B-D4 is the same as the eIF1A-binding surface (Fig. 4C).[4–6] NMR spectra of ^{15}N-labeled eIF5B-D4 with unlabeled eIF5-CT9 showed effects essentially indistinguishable from those with unlabeled eIF5-CT39 (compare Fig. S1A and B). Therefore, it appears that the dynamic contacts causing weak CSP effects in the internal portion of eIF5-CTT (Fig. 4A) do not cause significant effects on backbone NHs in eIF5B-D4. Binding of unlabeled eIF5-CTD to eIF5B-D4 affected the same residues, causing mostly identical CSP effects, except in the region near the N-terminal portion of eIF5B-D4, where the magnitude of the CSPs is slightly smaller with eIF5-CTD, compared to eIF5-CT9 (Fig. S1C).

The structure of the human eIF5B-D4•eIF5-CTT complex is very similar to that of the yeast eIF5B•eIF1A-CTT complex.

In the course of the NMR CSP experiments described above, it became clear that while free eIF5B-D4 and the eIF5B-D4•eIF1A complex have limited solubility, the eIF5B-D4•eIF5-CT39 complex is stable and soluble to at least 1 mM. We, therefore, proceeded to solve the structure of this complex by NMR. We used standard 3D triple-resonance NMR experiments[24–27] to obtain the backbone and sidechain resonance assignments of the complex. To obtain intra-molecular and inter-molecular distance restraints for the eIF5B-D4•eIF5-CT39 complex, we collected 3D ^{15}N-edited Nuclear Overhauser Effect Spectroscopy (NOESY) spectra. In NOESY spectra, magnetization is transferred through space and every pair of ^{1}H nuclei located < 5 Å apart gives rise to a peak. In a ^{15}N-edited spectrum, only peaks that involve a ^{1}H attached to a ^{15}N are observed. We collected a set of NOESY spectra on three different samples (Fig. S2A):

1) Both eIF5B-D4 and eIF5-CT39 15N-labeled. This spectrum yields both intra- and inter-molecular NOE peaks involving NH groups from either eIF5B-D4 or eIF5-CT39.

2) Both eIF5B-D4 and eIF5-CT39 ^{15}N-labeled, and eIF5B-D4 also perdeuterated. Since the proteins are dissolved in water, deuterium atoms in NH groups are exchanged back with ^{1}H, whereas the sidechains remain deuterated. In this spectrum, all sidechain NOE peaks are to sidechain 1H nuclei belonging to eIF5-CT39 (which is not deuterated). Therefore, all NOE peaks between eIF5-CT39 NHs and a sidechain ^{1}H are unambiguously **intra-**molecular, whereas all NOE peaks between eIF5B-D4 NHs and a sidechain ^{1}H are unambiguously **inter-**molecular.

3) Both eIF5B-D4 and eIF5-CT39 ^{15}N-labeled, and eIF5-CT39 also perdeuterated. In this spectrum all sidechain NOE peaks are to sidechain ^{1}H nuclei belonging to eIF5B-D4 (which is not deuterated). Therefore, all NOE peaks between eIF5-CT39 NHs and a sidechain ^{1}H are unambiguously **inter-**molecular, whereas all NOE peaks between eIF5B-D4 NHs and a sidechain ^{1}H are unambiguously **intra-**molecular.

This approach allowed us to reliably identify NOEs between eIF5B-D4 and eIF5-CT39 in the complex. Even though the CSP effects on eIF5-CT39 extended far from the C-terminus (Fig. 4A), NOE peaks to eIF5B-D4 were only observed for the C-terminal six residues of eIF5. The intermolecular NOEs we observed were fully compatible with the structure of the yeast eIF5B•eIF1A complex[5] (Fig. 4D and Fig. S2B), indicating that the two complexes are very similar, even at the atomic level. Therefore, we concluded that solving the atomic structure of the human eIF5B-D4•eIF5-CTT complex was not worthwhile since it would only yield marginal refinement of side-chain positions over the homology model shown in Figures 4D and S2B, and not produce any new biological information.

Discussion

A novel interaction between human eIF5 and eIF5B

In this work, we show that human eIF5 binds to eIF5B with sub-μM affinity (Table 1). This interaction provides an unexpected link between the two GTPases in translation initiation, eIF2 and eIF5B because eIF5 is the GAP of eIF2. The interaction is mediated by the C-terminus of eIF5, which is very similar to the C-terminus of eIF1A (Fig. 3) that also binds to eIF5B. Indeed, human eIF5 and eIF1A compete for binding to eIF5B-D4, with eIF5 having ~100-fold greater affinity (Table 1). The eIF5-CTT•eIF5B-D4 interface is very similar to the eIF1A-CTT•eIF5B-D4 interface (Fig. 4)[4–6] and involves hydrophobic, as well as electrostatic, interactions. While human eIF1A has only two hydrophobic residues contacting eIF5B (I140 and the C-terminal I143), eIF5 has three (I426, I428, and the C-terminal I431), all of which are involved in productive interactions (Fig. 4D). This difference likely accounts for the 10-fold higher affinity of the human eIF5-CTT, compared to the human eIF1A-CTT (Table 1). This makes the eIF5 C-terminus more similar to the *S. cerevisiae* eIF1A C-terminus, which also has three large hydrophobic residues at the same positions (Fig. 3), all contacting eIF5B.[5] Accordingly, while the affinity of yeast eIF1A for eIF5B is not known, it appears higher than that of human eIF1A because the interaction between the yeast proteins is strong enough to be observed by affinity pull-down.[23] Unlike

human eIF5, *S. cerevisiae* eIF5 does not have a C-terminal tail (Fig. 3) and is not known to bind to eIF5B. Comparison of our NMR results for the eIF5B-D4•eIF5-CTT complex with the crystal structure of the yeast eIF5B•eIF1A complex[5] shows that the two are remarkably similar (Fig. 4D and Fig. S2).

The eIF5B-binding motif in eIF5 was present in the last common ancestor of Eukaryotes

The eIF5B-binding motif is present in almost every known eIF1A sequence (a set of representative sequences is shown in Fig. 3). In contrast, our analysis shows that, while a C-terminal tail with an eIF5B-binding motif at the end is found in eIF5 proteins from most metazoan species, it is not as well conserved in other eukaryotes (Fig. 3). For example, no known plant eIF5 sequences have the eIF5B-binding motif and only a subset of fungal species, including *Ustilago maydis*, have a C-terminal tail with an eIF5B-binding motif. eIF5 sequences from species belonging to individual branches of other Kingdoms also have C-terminal tails with an eIF5B-binding motif (Fig. 3). Therefore, the eIF5B-binding C-terminus was present in the last common eukaryotic ancestor, but then lost in some kingdoms, and in parts of others. This observation indicates that eIF5-CTT could be taking over some of the eIF1A-CTT functions, but not others. The functions of eIF1A-CTT, and its interaction with eIF5B, in translation initiation, and the possible role of eIF5-CTT in the process are discussed below.

Function of the eIF5-CTT•eIF5B interaction

eIF1A and eIF5 bind to the same surface of eIF5B and compete with each other. It is, therefore, clear that the two interactions cannot occur simultaneously. The eIF1A•eIF5B interaction is important for ribosomal subunit joining, at the end of translation initiation. After formation of the 80S ribosome and GTP hydrolysis by eIF5B, eIF1A-CTT mediates the coordinated release of eIF1A and eIF5B from the ribosome.[21, 22] Binding of eIF1A to the ribosome removes the intramolecular interaction between the CTT and the OB domain, which exposes an eIF5B-binding surface on the eIF1A OB domain and also increases the eIF1A-CTT affinity for eIF5B.[6] However, when eIF1A binds to the 40S ribosomal subunit, its CTT is located in the ribosomal P-site, away from the eIF5B binding site on the 40S subunit. Upon start codon selection, the PIC undergoes a conformational transition from an open scanning-competent state to a closed state, accompanied by displacement of eIF1A-CTT from the P-site.[1–3] The eIF1A-CTT•eIF5B-D4 interaction is most likely established at that stage, because eIF1A-CTT is now able to reach the eIF5B position on the ribosome. In the 43S PIC, eIF1A can stabilize eIF5B binding to the ribosome through the eIF1A-OB•eIF5B-D3 interaction. Upon start codon recognition, the eIF1A-CTT•eIF5B-D4 interaction can also contribute to recruiting eIF5B to the 48S PIC, if it is not already bound, or to stabilize its binding.[6] Upon start codon selection, eIF5B accelerates the release of eIF2-GDP[20] and must be present in the PIC at that stage. eIF2-GDP is released from the ribosome in complex with eIF5.[16, 18, 19] Therefore, the eIF5-CTT•eIF5B-D4 interaction can take place before and until start codon selection. eIF5B has no known functions prior to start codon selection. Therefore, the most likely role of the eIF5-CTT•eIF5B interaction is recruitment of eIF5B to the 43S or 48S PIC, before it has reached the start codon. Since the binding affinity between free eIF1A and eIF5B off the ribosome is rather low due to competing intramolecular interactions,[6] it is unlikely for eIF1A and eIF5B to be recruited to the PIC as

a binary complex in human, although this is possible in *S. cerevisiae*, where the interaction seems to be stronger.[23] Even if eIF1A helps recruit eIF5B to the PIC, the eIF1A-CTT would not be able to stabilize eIF5B on the ribosome until after start codon selection. In contrast, human eIF5-CTT would be available for binding eIF5B in the 43S PIC, as well as during scanning. Unlike eIF1A, full-length human eIF5 has the same, or even higher affinity for eIF5B than eIF5-CTT (Table 1). This indicates that human eIF5 and eIF5B can form a complex off the ribosome and be recruited to the ribosome together. A multifactor Complex (MFC) was recently reported in human.[33] Therefore, human eIF5B could also be part of the MFC. This model is shown schematically in Fig. 5.

What are the potential benefits of early and stable recruitment of eIF5B to the PIC, through the interaction with eIF5-CTT? The obvious advantage is that this increases the probability of eIF5B already being present during start codon selection, even when most eIF5B is ribosome-bound and the concentration of free eIF5B in the cell is low. This would make translation initiation faster and more efficient, because the PIC would not have to stay idle until an eIF5B molecule binds, to help displace eIF2-GDP, and promote subunit joining. A delay in eIF5B binding to the PIC can have additional negative effects, beyond lower translation rate. Free Met-tRNA$_i$ is prone to deacylation,[34] which can happen if eIF2-GDP leaves the PIC before eIF5B is there to replace it. Subunit joining stabilizes the initiation complex at the start site and prevents it from sliding off. Therefore, delay in eIF5B binding and subunit joining increases the frequency of leaky scanning.[35–38] It is difficult to determine whether, or when, eIF5B binding to the PIC is rate-limiting because that depends on the binding rate constant and the concentration of free eIF5B, neither of which is known. A “best-case scenario” upper limit of the binding rate constant can be estimated assuming diffusion control and the intracellular concentrations of most translation initiation factors, including eIF5B, have been found to be in the low-μM range (see e.g. references [39, 40]); however, it is unclear what fraction of eIF5B is free at any given time, what fraction is bound to other PICs, or how this ratio varies with changes in the cell metabolic status. A cell can respond to slow rates of eIF5B binding to the PIC by increased steady-state eIF5B levels, or tolerate the associated drop in translation rates and rise in leaky scanning. Thus, while a role of the eIF5•eIF5B interaction in eIF5B recruitment to the PIC has obvious benefits, it does not appear essential, especially in simpler organisms. It is also possible that eIF5B plays additional, currently unknown roles in translation initiation before or during start codon selection.

Role of the competition between eIF5 and eIF1A for eIF5B

Since upon start codon selection, eIF1A-CTT becomes available to bind eIF5B and eIF5 leaves the PIC together with eIF2-GDP, at that stage, eIF1A-CTT must displace eIF5-CTT. This rearrangement is likely coordinated with eIF5B displacing eIF2-GDP from the Met-tRNA$_i$ (Fig. 5). The difference in affinity for eIF5B between eIF15-CTT and eIF1A-CTT is about ten-fold (Table 1). While this is not as great as the 100-fold difference of affinities between the full-length proteins, it is enough to raise the question how the weaker eIF1A-CTT•eIF5B-D4 interaction displaces the stronger eIF5-CTT•eIF5B-D4 interaction. A possible explanation is that the conformational rearrangements in the PIC could somehow lower the eIF5 affinity for eIF5B. eIF5-CTD has been reported to bind to eIF1, eIF1A,

eIF2β, and eIF3c, through multiple interaction interfaces that are partially overlapping and undergo major rearrangements during translation initiation.[23, 41–44] These findings indicate that while in binary eIF5:eIF2 complexes, eIF2β binds tightly to eIF5-CTD, in the scanning PIC, eIF2β is at least partially displaced by eIFs 1, 1A, and 3c. At the same time, the eIF5-CTD interaction with eIF3c prevents the latter from contacting the ribosome-binding surface of eIF1. Upon start codon selection, the PIC transition from an open scanning complex to a closed complex is accompanied by eIF2β displacing eIFs 1, 1A, and 3c from eIF5-CTD and release of eIF1 from the PIC.[41–43] It remains to be determined whether any of the interactions between eIF5-CTD and other eIFs affect the affinity of eIF5-CTT for eIF5B-D4. For instance, if eIF2β binding to eIF5-CTD weakens the eIF5 - eIF5B interaction, that would help eIF1A-CTT displace eIF5-CTT from the eIF5B-D4 surface. A second possibility is that changes in the positions and mutual orientation of eIF5B and eIF5 in the closed PIC could impair their ability to bind to each other. Even if the affinity between eIF5 and eIF5B is unaffected by ligands binding to eIF5-CTD, the location of eIF5-CTD is likely to change as a result of the structural rearrangements in the PIC upon start codon selection, and that could indirectly affect the ability of eIF5-CTT to reach eIF5B and bind to it, changing their effective concentrations in the vicinity of each other. Of course, these two possible explanations are not mutually exclusive.

More work needs to be done to elucidate the functions of the interaction between human eIF5 and eIF5B reported here, as well as the timing and molecular mechanisms of its formation and disruption during the process of translation initiation. In view of the role eIF5B plays in eIF2-independent translation initiation,[36, 45] the direct contact between eIF5 and eIF5B raises a set of new questions. Since eIF5 binds to eIF3 and eIF1, it could be present in these eIF2-independent PICs, either alone, or together with eIF2-GDP. It is currently not known whether eIF5 and/or eIF2 are present in such PICs, and if so, what roles they play.

Supplementary Material

Refer to Web version on PubMed Central for supplementary material.

Acknowledgments

Funding

This work was supported by the National Institutes of Health (grants GM095720 to AM and GM122602 to T.V.P.).

References

[1]. Martin-Marcos P, Cheung YN, and Hinnebusch AG (2011) Functional elements in initiation factors 1, 1A, and 2beta discriminate against poor AUG context and non-AUG start codons, Mol Cell Biol 31, 4814–4831. [PubMed: 21930786]

[2]. Nanda JS, Saini AK, Munoz AM, Hinnebusch AG, and Lorsch JR (2013) Coordinated movements of eukaryotic translation initiation factors eIF1, eIF1A, and eIF5 trigger phosphate release from eIF2 in response to start codon recognition by the ribosomal preinitiation complex, J Biol Chem 288, 5316–5329. [PubMed: 23293029]

[3]. Yu Y, Marintchev A, Kolupaeva VG, Unbehaun A, Veryasova T, Lai SC, Hong P, Wagner G, Hellen CU, and Pestova TV (2009) Position of eukaryotic translation initiation factor eIF1A on

the 40S ribosomal subunit mapped by directed hydroxyl radical probing, Nucleic Acids Res 37, 5167–5182. [PubMed: 19561193]

[4]. Marintchev A, Kolupaeva VG, Pestova TV, and Wagner G (2003) Mapping the binding interface between human eukaryotic initiation factors 1A and 5B: a new interaction between old partners, Proc Natl Acad Sci U S A 100, 1535–1540. [PubMed: 12569173]

[5]. Zheng A, Yu J, Yamamoto R, Ose T, Tanaka I, and Yao M (2014) X-ray structures of eIF5B and the eIF5B-eIF1A complex: the conformational flexibility of eIF5B is restricted on the ribosome by interaction with eIF1A, Acta Crystallogr D Biol Crystallogr 70, 3090–3098. [PubMed: 25478828]

[6]. Nag N, Lin KY, Edmonds KA, Yu J, Nadkarni D, Marintcheva B, and Marintchev A (2016) eIF1A/eIF5B interaction network and its functions in translation initiation complex assembly and remodeling, Nucleic acids research 44, 7441–7456. [PubMed: 27325746]

[7]. Asano K, Clayton J, Shalev A, and Hinnebusch AG (2000) A multifactor complex of eukaryotic initiation factors, eIF1, eIF2, eIF3, eIF5, and initiator tRNA(Met) is an important translation initiation intermediate in vivo, Genes Dev 14, 2534–2546. [PubMed: 11018020]

[8]. Asano K (2014) Why is start codon selection so precise in eukaryotes?, Translation (Austin) 2, e28387. [PubMed: 26779403]

[9]. Hinnebusch AG (2014) The scanning mechanism of eukaryotic translation initiation, Annu Rev Biochem 83, 779–812. [PubMed: 24499181]

[10]. Hinnebusch AG (2017) Structural Insights into the Mechanism of Scanning and Start Codon Recognition in Eukaryotic Translation Initiation, Trends Biochem Sci 42, 589–611. [PubMed: 28442192]

[11]. Hinnebusch AG, and Lorsch JR (2012) The mechanism of eukaryotic translation initiation: new insights and challenges, Cold Spring Harb Perspect Biol 4.

[12]. Jackson RJ, Hellen CU, and Pestova TV (2010) The mechanism of eukaryotic translation initiation and principles of its regulation, Nat Rev Mol Cell Biol 11, 113–127. [PubMed: 20094052]

[13]. Marintchev A, and Wagner G (2004) Translation initiation: structures, mechanisms and evolution, Q Rev Biophys 37, 197–284. [PubMed: 16194295]

[14]. Hershey JW, Sonenberg N, and Mathews MB (2012) Principles of translational control: an overview, Cold Spring Harb Perspect Biol 4.

[15]. Hinnebusch AG, Ivanov IP, and Sonenberg N (2016) Translational control by 5'-untranslated regions of eukaryotic mRNAs, Science 352, 1413–1416. [PubMed: 27313038]

[16]. Cheung YN, Maag D, Mitchell SF, Fekete CA, Algire MA, Takacs JE, Shirokikh N, Pestova T, Lorsch JR, and Hinnebusch AG (2007) Dissociation of eIF1 from the 40S ribosomal subunit is a key step in start codon selection in vivo, Genes Dev 21, 1217–1230. [PubMed: 17504939]

[17]. Kapp LD, and Lorsch JR (2004) GTP-dependent recognition of the methionine moiety on initiator tRNA by translation factor eIF2, J Mol Biol 335, 923–936. [PubMed: 14698289]

[18]. Singh CR, Lee B, Udagawa T, Mohammad-Qureshi SS, Yamamoto Y, Pavitt GD, and Asano K (2006) An eIF5/eIF2 complex antagonizes guanine nucleotide exchange by eIF2B during translation initiation, EMBO J 25, 4537–4546. [PubMed: 16990799]

[19]. Unbehaun A, Borukhov SI, Hellen CU, and Pestova TV (2004) Release of initiation factors from 48S complexes during ribosomal subunit joining and the link between establishment of codon-anticodon base-pairing and hydrolysis of eIF2-bound GTP, Genes Dev 18, 3078–3093. [PubMed: 15601822]

[20]. Pisarev AV, Kolupaeva VG, Pisareva VP, Merrick WC, Hellen CU, and Pestova TV (2006) Specific functional interactions of nucleotides at key −3 and +4 positions flanking the initiation codon with components of the mammalian 48S translation initiation complex, Genes Dev 20, 624–636. [PubMed: 16510876]

[21]. Acker MG, Shin BS, Dever TE, and Lorsch JR (2006) Interaction between eukaryotic initiation factors 1A and 5B is required for efficient ribosomal subunit joining, The Journal of biological chemistry 281, 8469–8475. [PubMed: 16461768]

[22]. Acker MG, Shin BS, Nanda JS, Saini AK, Dever TE, and Lorsch JR (2009) Kinetic analysis of late steps of eukaryotic translation initiation, J Mol Biol 385, 491–506. [PubMed: 18976658]

[23]. Olsen DS, Savner EM, Mathew A, Zhang F, Krishnamoorthy T, Phan L, and Hinnebusch AG (2003) Domains of eIF1A that mediate binding to eIF2, eIF3 and eIF5B and promote ternary complex recruitment in vivo, EMBO J 22, 193–204. [PubMed: 12514125]

[24]. Bax A, Ikura M, Kay LE, Barbato G, and Spera S (1991) Multidimensional triple resonance NMR spectroscopy of isotopically uniformly enriched proteins: a powerful new strategy for structure determination, Ciba Found Symp 161, 108–119; discussion 119–135. [PubMed: 1814691]

[25]. Ikura M, Krinks M, Torchia DA, and Bax A (1990) An efficient NMR approach for obtaining sequence-specific resonance assignments of larger proteins based on multiple isotopic labeling, FEBS Lett 266, 155–158. [PubMed: 2114317]

[26]. Kanelis V, Forman-Kay JD, and Kay LE (2001) Multidimensional NMR methods for protein structure determination, IUBMB Life 52, 291–302. [PubMed: 11895078]

[27]. Montelione GT, and Wagner G (1990) Triple resonance experiments for establishing conformation-independent sequential NMR assignments in isotope-enriched polypeptides, J Magn Res 87, 183–188.

[28]. Altschul SF, Madden TL, Schaffer AA, Zhang J, Zhang Z, Miller W, and Lipman DJ (1997) Gapped BLAST and PSI-BLAST: a new generation of protein database search programs, Nucleic Acids Res 25, 3389–3402. [PubMed: 9254694]

[29]. Larkin MA, Blackshields G, Brown NP, Chenna R, McGettigan PA, McWilliam H, Valentin F, Wallace IM, Wilm A, Lopez R, Thompson JD, Gibson TJ, and Higgins DG (2007) Clustal W and Clustal X version 2.0, Bioinformatics 23, 2947–2948. [PubMed: 17846036]

[30]. Thompson JD, Higgins DG, and Gibson TJ (1994) CLUSTAL W: improving the sensitivity of progressive multiple sequence alignment through sequence weighting, position-specific gap penalties and weight matrix choice, Nucleic Acids Res 22, 4673–4680. [PubMed: 7984417]

[31]. Pestova TV, Lomakin IB, Lee JH, Choi SK, Dever TE, and Hellen CU (2000) The joining of ribosomal subunits in eukaryotes requires eIF5B, Nature 403, 332–335. [PubMed: 10659855]

[32]. Battiste JL, Pestova TV, Hellen CU, and Wagner G (2000) The eIF1A solution structure reveals a large RNA-binding surface important for scanning function, Mol Cell 5, 109–119. [PubMed: 10678173]

[33]. Sokabe M, Fraser CS, and Hershey JW (2012) The human translation initiation multi-factor complex promotes methionyl-tRNA$_i$ binding to the 40S ribosomal subunit, Nucleic acids research 40, 905–913. [PubMed: 21940399]

[34]. Yatime L, Schmitt E, Blanquet S, and Mechulam Y (2004) Functional molecular mapping of archaeal translation initiation factor 2, J Biol Chem 279, 15984–15993. [PubMed: 14761973]

[35]. Lee JH, Pestova TV, Shin BS, Cao C, Choi SK, and Dever TE (2002) Initiation factor eIF5B catalyzes second GTP-dependent step in eukaryotic translation initiation, Proceedings of the National Academy of Sciences of the United States of America 99, 16689–16694. [PubMed: 12471154]

[36]. Pestova TV, de Breyne S, Pisarev AV, Abaeva IS, and Hellen CU (2008) eIF2-dependent and eIF2-independent modes of initiation on the CSFV IRES: a common role of domain II, EMBO J 27, 1060–1072. [PubMed: 18337746]

[37]. Pestova TV, and Kolupaeva VG (2002) The roles of individual eukaryotic translation initiation factors in ribosomal scanning and initiation codon selection, Genes Dev 16, 2906–2922. [PubMed: 12435632]

[38]. Pisareva VP, and Pisarev AV (2014) eIF5 and eIF5B together stimulate 48S initiation complex formation during ribosomal scanning, Nucleic Acids Res 42, 12052–12069. [PubMed: 25260592]

[39]. von der Haar T, and McCarthy JE (2002) Intracellular translation initiation factor levels in Saccharomyces cerevisiae and their role in cap-complex function, Mol Microbiol 46, 531–544. [PubMed: 12406227]

[40]. Wang M, Weiss M, Simonovic M, Haertinger G, Schrimpf SP, Hengartner MO, and von Mering C (2012) PaxDb, a database of protein abundance averages across all three domains of life, Mol Cell Proteomics 11, 492–500. [PubMed: 22535208]

[41]. Luna RE, Arthanari H, Hiraishi H, Akabayov B, Tang L, Cox C, Markus MA, Luna LE, Ikeda Y, Watanabe R, Bedoya E, Yu C, Alikhan S, Wagner G, and Asano K (2013) The interaction between eukaryotic initiation factor 1A and eIF5 retains eIF1 within scanning preinitiation complexes, Biochemistry 52, 9510–9518. [PubMed: 24319994]

[42]. Luna RE, Arthanari H, Hiraishi H, Nanda J, Martin-Marcos P, Markus MA, Akabayov B, Milbradt AG, Luna LE, Seo HC, Hyberts SG, Fahmy A, Reibarkh M, Miles D, Hagner PR, O'Day EM, Yi T, Marintchev A, Hinnebusch AG, Lorsch JR, Asano K, and Wagner G (2012) The C-terminal domain of eukaryotic initiation factor 5 promotes start codon recognition by its dynamic interplay with eIF1 and eIF2beta, Cell Rep 1, 689–702. [PubMed: 22813744]

[43]. Obayashi E, Luna RE, Nagata T, Martin-Marcos P, Hiraishi H, Singh CR, Erzberger JP, Zhang F, Arthanari H, Morris J, Pellarin R, Moore C, Harmon I, Papadopoulos E, Yoshida H, Nasr ML, Unzai S, Thompson B, Aube E, Hustak S, Stengel F, Dagraca E, Ananbandam A, Gao P, Urano T, Hinnebusch AG, Wagner G, and Asano K (2017) Molecular Landscape of the Ribosome Pre-initiation Complex during mRNA Scanning: Structural Role for eIF3c and Its Control by eIF5, Cell Rep 18, 2651–2663. [PubMed: 28297669]

[44]. Reibarkh M, Yamamoto Y, Singh CR, del Rio F, Fahmy A, Lee B, Luna RE, Ii M, Wagner G, and Asano K (2008) Eukaryotic initiation factor (eIF) 1 carries two distinct eIF5-binding faces important for multifactor assembly and AUG selection, The Journal of biological chemistry 283, 1094–1103. [PubMed: 17974565]

[45]. Terenin IM, Dmitriev SE, Andreev DE, and Shatsky IN (2008) Eukaryotic translation initiation machinery can operate in a bacterial-like mode without eIF2, Nat Struct Mol Biol 15, 836–841. [PubMed: 18604219]

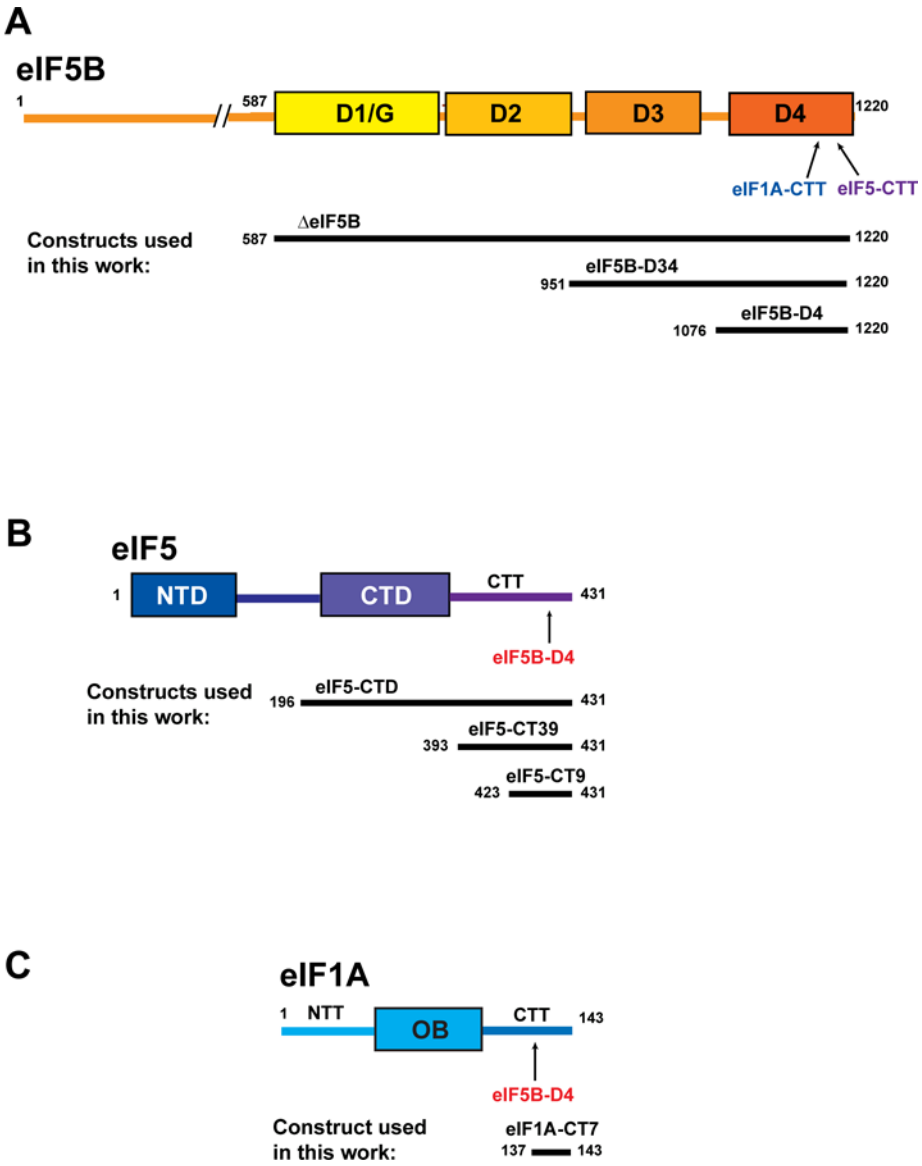

Figure 1. Domain structure and interactions of eIF5B, eIF5, and eIF1A.

(A) Top, domain structure of eIF5B. The binding site for eIF1A-CTT and eIF5-CTT is labeled. ***Bottom***, constructs used in this work. **(B)** ***Top***, domain structure of eIF5. The binding site for eIF5B-D4 is labeled. ***Bottom***, constructs used in this work. **(C)** ***Top***, domain structure of eIF1A. The binding site for eIF5B-D4 is labeled. ***Bottom***, construct used in this work.

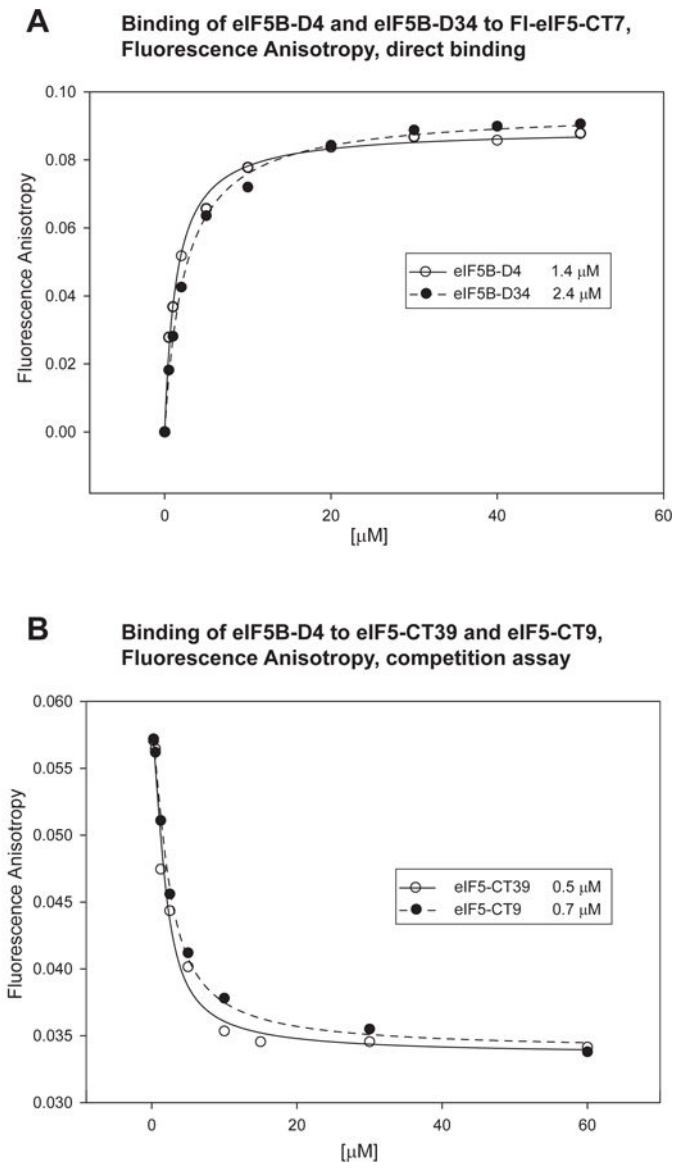

Figure 2. Binding affinities between eIF5 and eIF5B fragments determined by fluorescence anisotropy (FA).

(A) Direct titration of fluorescein-labeled 7-residue eIF5 C-terminal peptide (Fl-eIF5-CT7) with eIF5B domain 4 (eIF5B-D4) and eIF5B domains 3 and 4 (eIF5B-D34). The calculated K_Ds are shown in the inset. **(B)** Competition assay with eIF5-CT9 and eIF5-CT39. The calculated K_Ds are shown in the inset.

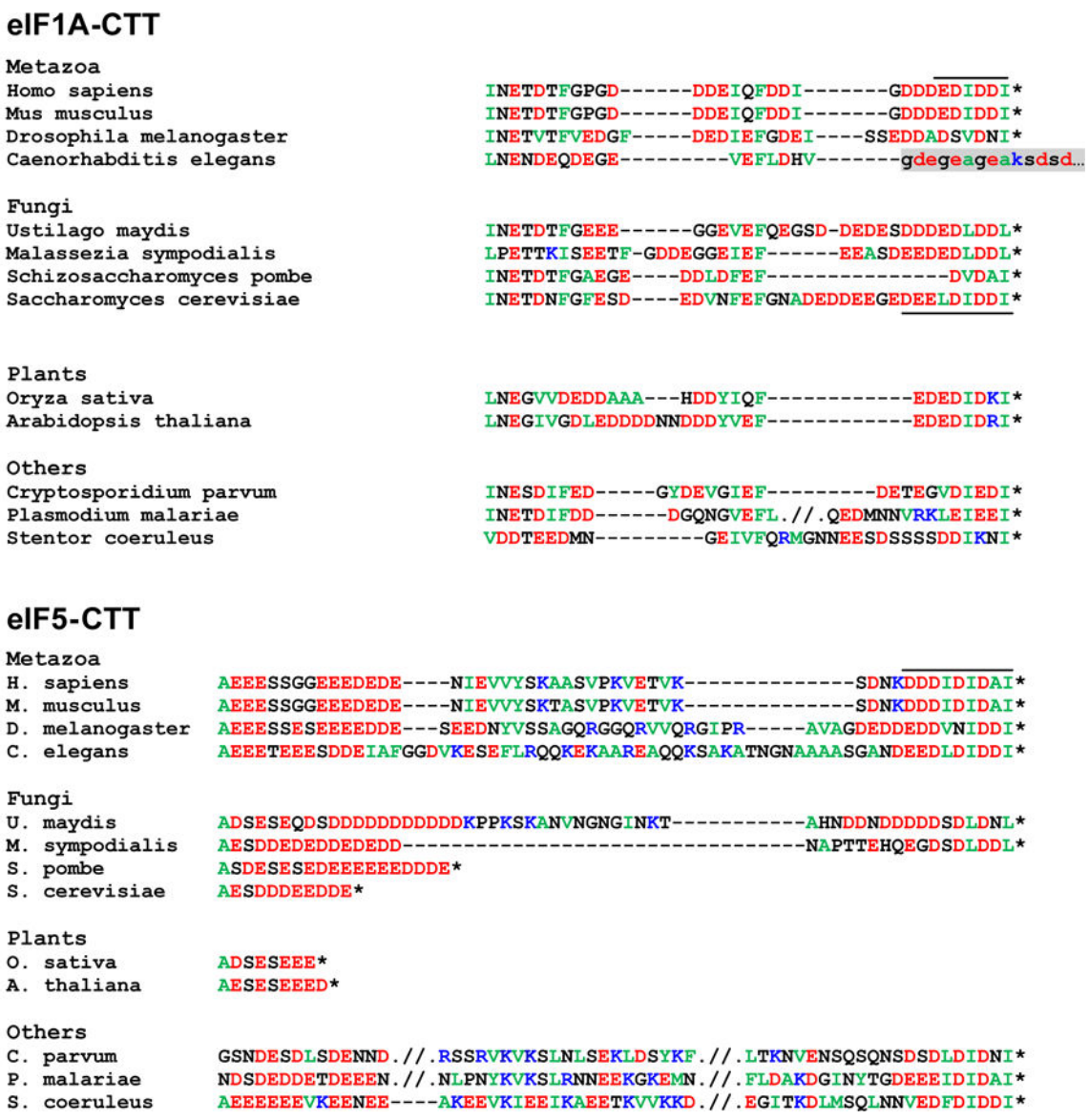

Figure 3. The C-termini of eIF1A and eIF5 are conserved.

Sequence alignment of eIF1A (***top***) and eIF5 (***bottom***) C-terminal tail (CTT) sequences from a select set of species. Hydrophobic residues are green; negatively charged residues are red, and positively charged residues are blue. The C-termini of the proteins are marked with *. Locations of intervening sequences not included in the alignment are marked with //. The eIF5B-binding motifs at the C-terminus of human[4] and *S. cerevisiae*[5] eIF1A, and human eIF5 (this work) are marked with a line. The eIF5B-binding motif is conserved in eIF5 from *Metazoa*, as well as fungi from subphylum *Ustilaginomycotina.* It is not found in eIF5 from other fungal species, including budding and fission yeast, or in plant eIF5. The C-terminus of metazoan eIF5 appears more similar to that of *S. cerevisiae* eIF1A than human eIF1A. eIF1A-CTT and eIF5-CTT from *Ustilaginomycotina* fungi appear more similar to each other than to eIF1A or eIF5 sequences from other species. The C-terminal sequence of *C. elegans*

eIF1A (in lower-case and highlighted gray) does not appear to contain an eIF5B-binding motif.

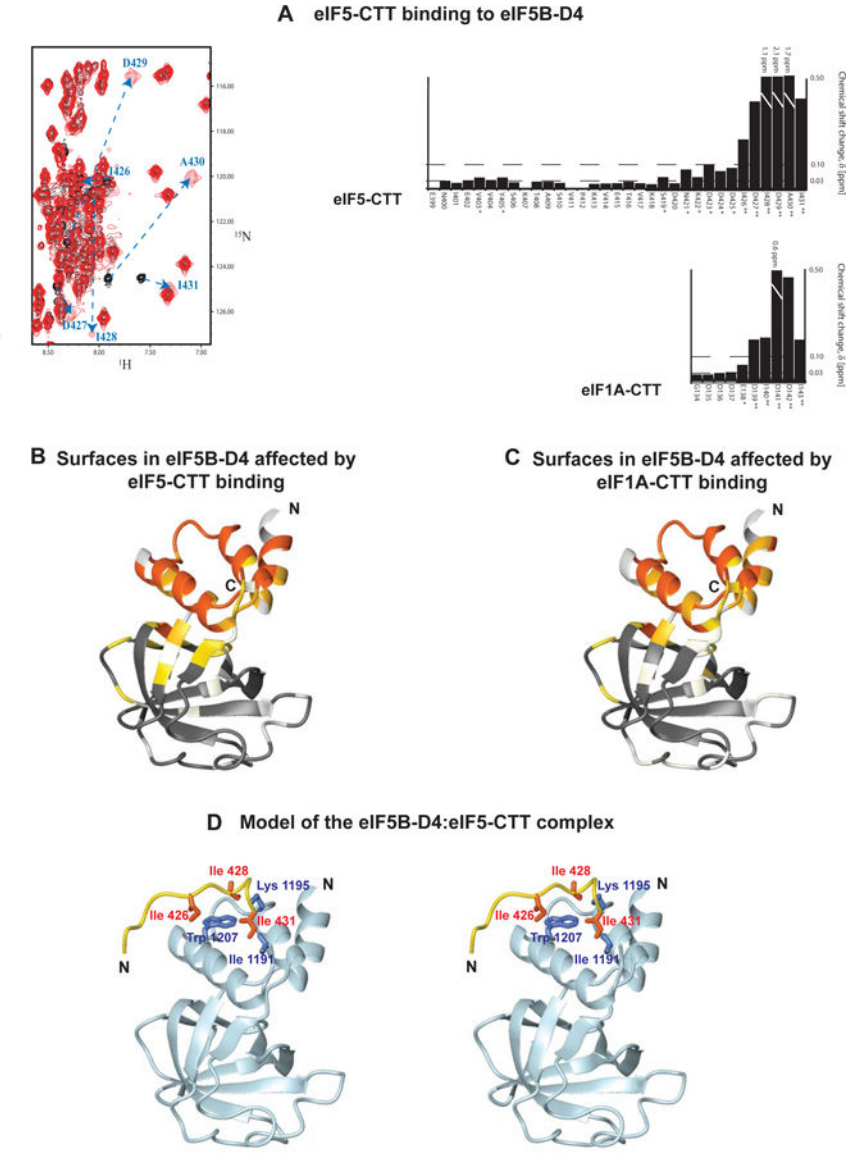

Figure 4. Comparison of the eIF5B•eIF5 and eIF5B•eIF1A binding interfaces

(A) Comparison of eIF5B-D4 binding to eIF5-CTT and eIF1A. ***Left***, region of the ^{15}N-HSQC spectra of GB1-tagged eIF5-CT39 (GH-eIF5-CT39) in the absence (black) and presence (red) of unlabeled eIF5B-D4. The C-terminal six residues of eIF5 are labeled and the changes in their positions upon binding of eIF5B-D4 are marked with dashed arrows. ***Right***, eIF5B-D4 induced chemical shift perturbation (CSP) mapped on the sequence of eIF5-CTT (***top***) and eIF1A-CTT (***bottom***, from reference [4]). Only the last 10 residues of eIF1A and the last 33 residues of eIF5 are shown, because there were no detectable CSP effects on the rest of the two tails. Residues experiencing medium (>0.03 ppm) and large (>0.1 ppm) CSP effects are marked with * and **, respectively. **(B)** eIF5-CTT binding surface of eIF5B-D4. eIF5-CTT induced CSPs were mapped on the structure of human eIF5B-D4, from light yellow (weak effects) to red (strong effects). Residues that could not be analyzed are light grey. **(C)** eIF1A-CTT binding surface of eIF5B-D4 from reference *6*

shown for comparison. Coloring is as in panel *B*. **(D)** Model of the human eIF5B-D4•eIF5-CTT complex, in cross-eye stereo, based on the yeast eIF5B-D4•eIF1A-CTT complex.[5] eIF5B-D4 is light blue, and eIF5-CTT is gold. Sidechains exhibiting intermolecular NOEs between eIF5 and eIF5B, are shown as blue (eIF5B) and red (eIF5) sticks, and the corresponding residues are labeled.

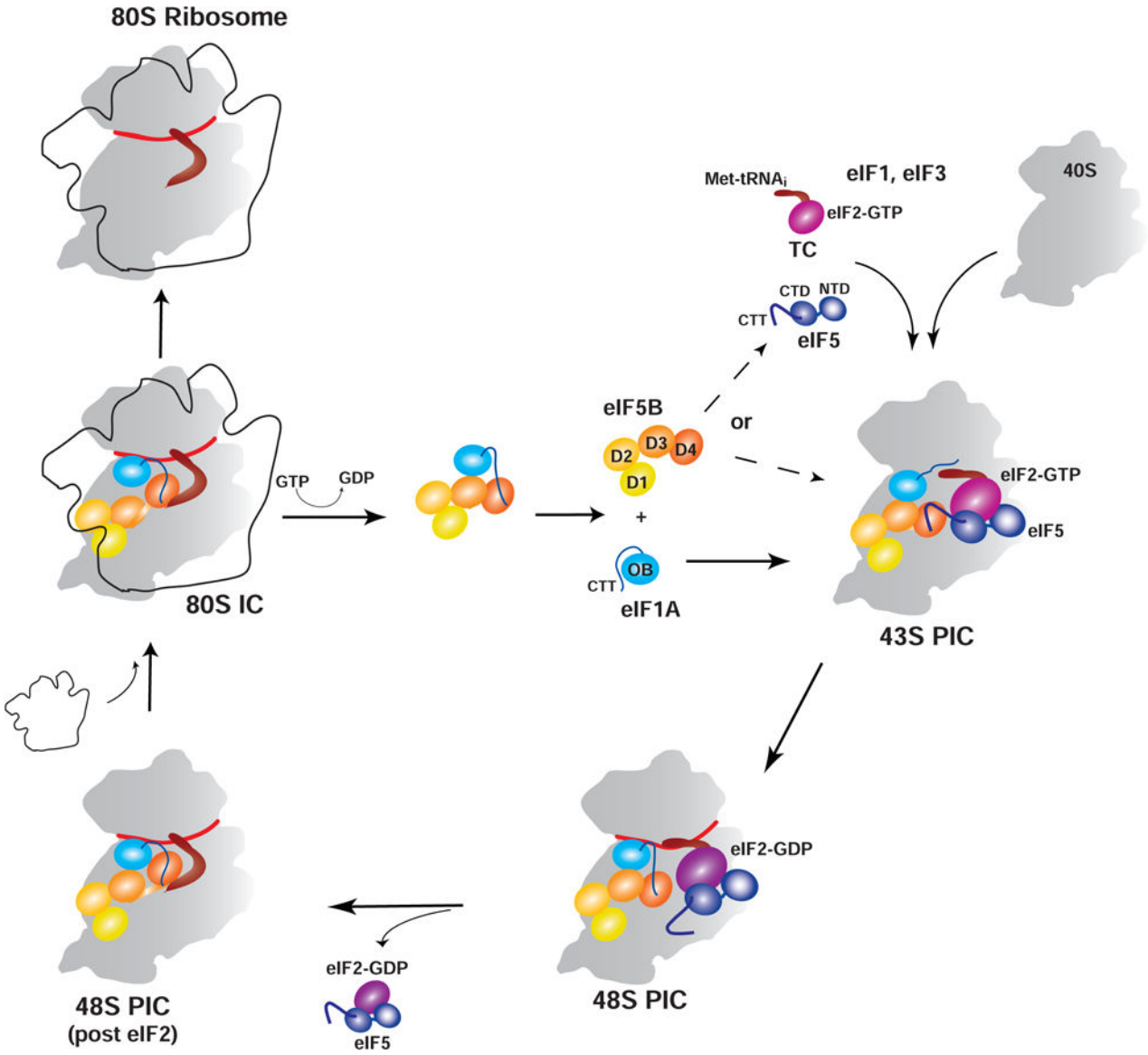

Figure 5. Model for the dynamic interactions of human eIF5 and eIF1A with eIF5B.

eIF5 is navy. The coloring of eIF5B is from yellow (D1) to dark orange (D4); the N-terminal region of eIF5B is not shown. eIF1A-OB is light blue; eIF1A-CTT is blue; and eIF1A-NTT is not shown. eIF2-GTP is magenta; eIF2-GDP is purple. The 40S ribosomal subunit is gray. The 60S ribosomal subunit is shown as an outline. The alternative pathways for eIF5B recruitment to the 43S PIC are marked with dashed arrows. eIF5B may either bind directly to the PIC through interactions with eIF5, the 40S subunit, and eIF1A-OB, or be recruited in complex with eIF5, possibly as a component of the multifactor complex (MFC). In the scanning PIC, eIF1A-CTT extends into the P-site, where it stabilizes the open complex. Start codon recognition promotes the closed, scanning-incompetent conformation of the PIC; eIF1A-CTT is displaced from the P-site[1–3] and in turn displaces eIF5-CTT from eIF5B-D4. This process is likely coupled to eIF5B displacing eIF2-GDP from the Met-tRNA$_i$, which leads to release of the eIF5•eIF2-GDP complex from the 48S PIC.

Table 1.

Binding affinities between eIF5 and eIF5B constructs, determined by Fluorescence Anisotropy (FA)

	eIF5B-D4 (μM)	eIF5B-D34 (μM)
Fl-eIF5-CT7[1]	1.4 +/− 0.1	2.4 +/− 0.1
eIF5-CT9[2]	0.74 +/− 0.08	1.2 +/− 0.2
eIF5-CT39[2]	0.5 +/− 0.1	1.1 +/− 0.2
eIF5-CTD[2]	0.37 +/− 0.06	0.72 +/− 0.09
eIF5[2]	0.37 +/− 0.07	0.51 +/− 0.09
Fl-eIF1A-CT7[3]	12 ± 1	27 ± 3
eIF1A-CTT[3]	12 ± 2	18 ± 5
eIF1A[3]	39 ± 9	41 ± 9

[1] Direct binding FA assay to fluorescein-labeled synthetic eIF5-CT7 peptide (Fl-eIF5-CT7)

[2] Competition FA assay

[3] From reference *6*.